



Primordial noble gases in a graphite-metal inclusion from the Canyon Diablo IAB iron meteorite and their implications

Jun-ichi MATSUDA,^{1*} Miwa NAMBA,¹ Teruyuki MARUOKA,^{1†} Takuya MATSUMOTO,¹ and Gero KURAT²

¹Department of Earth and Space Science, Graduate School of Science, Osaka University, Toyonaka, Osaka 560–0043, Japan

²Institut für Geologische Wissenschaften, Universität Wien, Althanstrasse 14, A-1090 Vienna, Austria

[†]Present address: Graduate School of Life and Environmental Sciences, University of Tsukuba, Tsukuba, Ibaraki 305–8572, Japan

*Corresponding author. E-mail: matsuda@ess.sci.osaka-u.ac.jp

(Received 01 July 2004; revision accepted 29 December 2004)

Abstract—We have carried out noble gas measurements on graphite from a large graphite-metal inclusion in Canyon Diablo. The Ne data of the low-temperature fractions lie on the mixing line between air and the spallogenic component, but those of high temperatures seem to lie on the mixing line between Ne-HL and the spallogenic component. The Ar isotope data indicate the presence of Q in addition to air, spallogenic component and Ar-HL. As the elemental concentration of Ne in Q is low, we could not detect the Ne-Q from the Ne data. On the other hand, we could not observe Xe-HL in our Xe data. As the Xe concentration and the Xe/Ne ratio in Q is much higher than that in the HL component, it is likely that only the contribution of Q is observed in the Xe data. Xenon isotopic data can be explained as a mixture of Q, air, and “El Taco Xe.” The Canyon Diablo graphite contains both HL and Q, very much like carbonaceous chondrites, retaining the signatures of various primordial noble gas components. This indicates that the graphite was formed in a primitive nebular environment and was not heated to high, igneous temperatures. Furthermore, a large excess of ¹²⁹Xe was observed, which indicates that the graphite was formed at a very early stage of the solar system when ¹²⁹I was still present. The HL/Q ratios in the graphite in Canyon Diablo are lower than those in carbonaceous chondrites, indicating that some thermal metamorphism occurred on the former. We estimated the temperature of the thermal metamorphism to about 500–600 °C from the difference of thermal retentivities of HL and Q. It is also noted that “El Taco Xe” is commonly observed in many IAB iron meteorites, but its presence in carbonaceous chondrites has not yet been established.

INTRODUCTION

The elemental abundances and the isotopic compositions of noble gases in meteorites have been studied to examine the origin and evolution of our solar system. Especially, the primordial components of noble gases in meteorites are very useful to get information on the formation mechanisms of meteorites. Iron meteorites, one class of differentiated meteorites, contain very small amounts of primordial noble gases which are generally masked by a large amount of spallogenic noble gases produced by cosmic ray irradiation. Thus, it has been very difficult to obtain precise data on primordial components of noble gases in iron meteorites, but they obviously are very important for understanding the origin of meteorites. In contrast, inclusions in iron meteorites generally contain large amounts of primordial noble gases. Some inclusions such as graphite and troilite were shown to

contain large amounts of primordial gases as compared to the metal phase (e.g., Alexander and Manuel 1967; Hwaung and Manuel 1982; Mathew and Begemann 1995). It is likely, as some of the iron meteorites such as the IAB, IIICD, and IIE irons are supposed to be of non-magmatic origin (Scot and Wasson 1975; Wasson and Wang 1986), that primordial noble gases were collected and retained by these iron meteorites.

Alexander and Manuel (1967, 1968) measured the elemental abundances and isotopic compositions of noble gases in a graphite nodule from the Canyon Diablo IAB iron meteorite. Unfortunately, the data on light noble gases turned out to be largely obscured by spallogenic components. However, there were clear excesses of ⁸⁰Kr and ⁸²Kr which were attributed to the neutron irradiation on bromine, and there was a large excess of ¹²⁹Xe, the decay product of the extinct nuclide ¹²⁹I. Their data on heavy noble gases were of sufficient quality for a discussion of spallogenic and

radiogenic components, but were not good enough to render precise information on the primordial noble gas component itself. Furthermore, the various components of noble gases such as Q (a normal component enriched in heavy noble gases in an unknown carrier), HL (a component enriched in heavy and light isotopes of Xe in presolar diamonds), etc. had not been established at that time. Recently, Namba et al. (2000) performed noble gas analyses of a carbon residue of the Canyon Diablo iron meteorite, but meaningful data have been obtained only for Ne isotopes.

Manuel's group (Hwaung and Manuel 1982; Hennecke and Manuel 1977) and Shukolyukov et al. (1984) reported that there might be a terrestrial atmosphere-like component in iron meteorites. If this is true, it is very important for any model on the formation of iron meteorites, but it is likely that this air component is a contamination acquired during sample preparation and measurement (Fisher 1981; Matsuda et al. 1996). Mathew and Begemann (1995) reported that graphite inclusions from the El Taco mass of the Campo del Cielo IAB iron meteorite contain a new noble gas end member. The Xe data obtained from silicate inclusions plot on a mixing line between air and the ureilite data points, but those from graphite were on the mixing line between air and a new component named "El Taco Xe." It was suggested that El Taco Xe was further separable into two components and was redefined based on ^{132}Xe -normalization of the data (Maruoka 1999). El Taco Xe is also observed in the Bohumilitz and Toluca IAB iron meteorites (Maruoka et al. 2001).

This time we had the opportunity to analyze a very large graphite-metal inclusion CDGrMet (Fig. 1; No. 7192, MPA, Naturhistorisches Museum, Vienna) from the Canyon Diablo IAB iron meteorite (Kurat et al. 2000). The graphite-metal inclusion CDGrMet consists of a porous aggregation of platy, spherulitic, vermicular and botryoidal graphite cut by shrinkage veins filled by metal and graphite (see also Kurat et al. 2000). The pores between individual graphite objects are filled by kamacite, rust, sulfides, schreibersite and silicates (enstatite, albite, and forsterite). Tiny pores inside cliftonite graphite are open. Rust is abundant, is rich in Cl and develops quickly on freshly cut surfaces (probably from lawrencite), especially along thin veins and at some graphite-metal grain boundaries. Veins of varying sizes have also varying properties. Very large veins (>300 μm thick) contain mainly granular kamacite and abundant cliftonite with some schreibersite and taenite and rare sulfide. Medium-sized veins (<100 μm thick) are filled by graphite-kamacite intergrowths which are oriented perpendicular to the vein walls. Thin veins (<50 μm thick) in part also consist of similar metal-graphite intergrowths, but contain mostly rust and some relict kamacite.

In order to investigate the primordial components in iron meteorites, we have measured the elemental abundances and isotopic compositions of all noble gases in graphite in this large graphite-metal inclusion. The gases were released in several temperature steps.

SAMPLE PREPARATION AND MEASUREMENTS OF NOBLE GASES

We broke this graphite-metal inclusion into small pieces and treated one of them with HCl to remove the metal portion. We put 594.18 mg of the inclusion in 6M HCl overnight at room temperature six times, heated it with 12M HCl overnight at 65 °C three times, and then boiled it with 12M HCl for one hour three times. We washed the graphite sample repeatedly until the supernatant fluid had a neutral pH. The remained sample was 371.06 mg and was named "CG1." We used 359.97 mg of CG1 for the noble gas measurement. The elemental abundances and isotopic compositions of noble gases have been measured with the mass spectrometer VG5400 installed at Osaka University.

The noble gas extractions and measurements were carried out by heating the sample in seven steps from 600 to 1800 °C with an interval of 200 °C, and finally again at 1800 °C. Unfortunately, we could not get the Xe data of the first 1800 °C heating step because of a failure of the peak detection routine of the computer software. The details of our experimental procedures are given in our previous works (Matsuda et al. 1989; Maruoka et al. 2001; Amari et al. 2003). The hot blank at 800 °C was applied for the sample gas measured at 600 and 800 °C and that at 1800 °C for the other temperature steps. The amounts and isotopic compositions of hot blanks are given with the obtained data in Tables 1–3. The ^3He blanks were not detected. The isotopic ratios of Ar and Kr blanks are nearly atmospheric, and we used the atmospheric ratios for Xe blanks. The blank corrections did not have large effects on Xe isotopes, where even the highest blank correction was at most 5%. The blank corrections for He, Ar, and Kr were also negligible in almost all the temperature fractions except for the highest temperature fractions. The isotopic ratios of Ne blanks were very much different from air values. This is due to the large interference of doubly charged $^{44}\text{CO}_2$, $^{40}\text{Ar}^+$ and CO_2^+ peaks were monitored during the Ne analyses. Since the $^{40}\text{Ar}^{++}$ peak could be partly resolved from $^{20}\text{Ne}^+$ with our mass spectrometer resolution of about 600, we chose a field position on the flat peak of $^{20}\text{Ne}^+$ that is free from $^{40}\text{Ar}^{++}$. Meanwhile, the amount of background CO_2 was fairly constant for the blanks and the sample measurements, the correction for the effect of CO_2^{++} on $^{22}\text{Ne}^+$ was included in the blank correction. The blank corrections to Ne isotopes were fairly large at high temperature fractions, and these corrections tend to give ratios higher than the measured ones, which will be important to discuss for the Ne data later.

RESULTS AND DISCUSSION

The results are listed in Tables 1–3. The errors of noble gas elemental abundances are less than 5% including all the errors of the line volume, standard air, etc., except for the total Xe, the concentration error of which is estimated to be about 10% because we lost the first step of the 1800 °C release. The

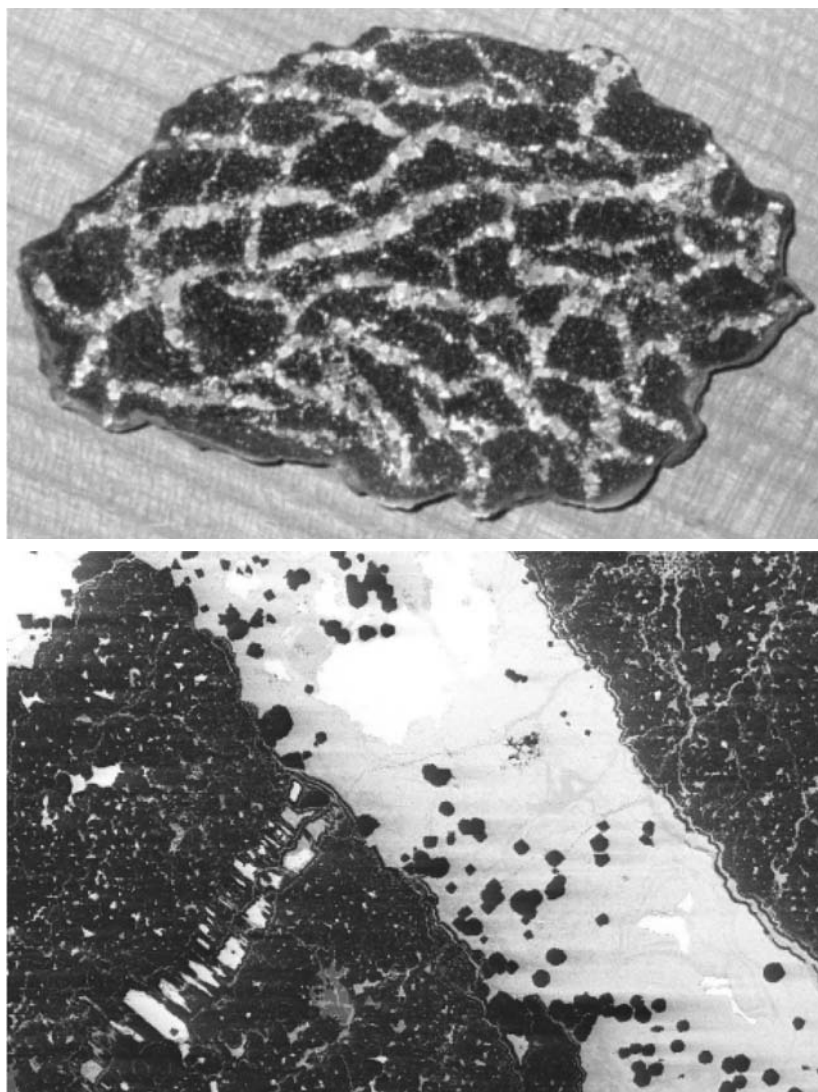


Fig. 1. a) Plate cut from the huge graphite-metal inclusion CDGrMet from Canyon Diablo (No. 7192, MPA, Naturhistorisches Museum, Vienna). Veins cutting through graphite are filled by granular Fe-Ni metal (gray). Note also the finely dispersed metal in the graphite. Length of the sample is 8.5 cm. b) Detail of graphite-metal inclusion (CDGrMet5) depicting a large metal vein (gray to white) containing abundant cliftonite graphite (black) and a medium-size vein (from center to lower left corner) consisting of graphite-metal intergrowths oriented perpendicular to the vein's walls. Note also the botryoidal habit of graphite in the matrix with inter-graphite voids filled by metal (white), sulfides, rust, and silicates (gray). Length of BSE image is 2 mm.

errors in the isotopic ratios include all the errors of the mass discrimination factor and hot blanks correction. The data of terrestrial atmosphere, Q and HL (and "El Taco Xe") are also listed in the tables for comparison.

Neon and Helium

The Ne isotopic data are plotted on a three-isotope diagram (Fig. 2). The data points for the 600–1200 °C fractions of CG1 are located on a mixing line between air and Ne-S (spallogenic component; Mazor et al. 1970), and those for the 1400 and 1600 °C fractions seem to lie on the mixing line between Ne-HL (Ne-A2) and Ne-S. Although we assumed the spallogenic composition (Ne-S) as a single

component from Mazor et al. (1970), the $^{21}\text{Ne}/^{22}\text{Ne}$ ratios of the spallogenic component range from 0.8 to 1.0 in iron meteorites (Schultz and Kruse 1989). Here, it is noted that even if the $^{21}\text{Ne}/^{22}\text{Ne}$ of Ne-S is as low as 0.8, the Ne data of the highest temperature fraction (1600 °C) seem to be situated slightly below the mixing line of Ne-S and air. This is not due to the artifact of the blank correction. Because the $^{20}\text{Ne}/^{22}\text{Ne}$ ratios of the hot blanks are as low as 1.65 and 2.41 (Table 1), the blank corrections make the corrected $^{20}\text{Ne}/^{22}\text{Ne}$ ratios higher than the raw measured ones. We routinely measure hot blanks. The blank data used in this study were the ones measured just before the sample measurements. The amounts of hot blanks tend to decrease with increasing time, so we believe that the low $^{20}\text{Ne}/^{22}\text{Ne}$ ratios in 1400 and 1600 °C

Table 1. Helium, Ne, and Ar in graphite nodule CG1 (359.97 mg) of Canyon Diablo.

Sample	Temp. (°C)	[⁴ He] ^a	³ He/ ⁴ He (×10 ⁻⁴)	[²⁰ Ne] ^a	²⁰ Ne/ ²² Ne	²¹ Ne/ ²² Ne	[³⁶ Ar] ^a	³⁸ Ar/ ³⁶ Ar	⁴⁰ Ar/ ³⁶ Ar
CG1	600	2.6	41.0 ± 105	2.0	9.785 ± 0.040	0.03511 ± 0.00056	11	0.18677 ± 0.00027	275.7 ± 2.4
	800	0.30	102.6 ± 3.7	0.28	9.017 ± 0.064	0.0975 ± 0.0013	2.7	0.18878 ± 0.00027	276.9 ± 2.4
	1000	0.17	31.9 ± 1.1	0.12	7.646 ± 0.064	0.2324 ± 0.0033	4.3	0.18889 ± 0.00029	217.1 ± 1.9
	1200	0.30	5.05 ± 0.18	0.0098	6.54 ± 0.25	0.389 ± 0.010	1.7	0.19200 ± 0.00031	82.68 ± 0.72
	1400			0.0030	4.74 ± 0.29	0.464 ± 0.020	1.2	0.19340 ± 0.00029	47.83 ± 0.42
	1600			0.0016	6.14 ± 0.95	0.202 ± 0.034	0.98	0.19209 ± 0.00033	36.45 ± 0.32
	1800-1						0.64	0.18983 ± 0.00033	31.05 ± 0.27
	1800-2						0.25	0.18713 ± 0.00044	22.67 ± 0.20
total		3.4	42.7 ± 1.5	2.4	9.520 ± 0.035	0.0586 ± 0.0012	23	0.18844 ± 0.00015	219.3 ± 1.4
Q ^b			1.59		10.70	<0.318		1.1875	<0.08
HL ^c			1.7		8.50	0.036		0.2270	0
Terrestrial air			0.014		9.8	0.029		0.188	295.5

Table 1a. Noble gas amounts and isotopic ratios of hot blanks.

Sample	Temp. (°C)	[⁴ He] (×10 ⁻¹⁰ cm ³ STP)	³ He/ ⁴ He	[²⁰ Ne] (×10 ⁻¹² cm ³ STP)	²⁰ Ne/ ²² Ne	²¹ Ne/ ²² Ne	[³⁶ Ar] (×10 ⁻¹¹ cm ³ STP)	³⁸ Ar/ ³⁶ Ar	⁴⁰ Ar/ ³⁶ Ar
800	4.5	0	0	3.6	1.65 ± 0.15	0.00325 ± 0.00192	0.76	0.1795 ± 0.0026	266.6 ± 2.6
1800	3.8	0	0	5.1	2.41 ± 0.12	0.00423 ± 0.00072	5.1	0.1881 ± 0.0011	271.8 ± 2.4

^aGas concentrations are in units of 10⁻⁸ cm³STP/g.^bWieler et al. (1991) for He and Ne; Huss et al. (1996) and Huss and Lewis (1994a) for Ar.^cHuss and Lewis (1994b).

Table 2. Krypton in graphite nodule CG1 (359.97 mg) of Canyon Diablo.

Sample	Temp. (°C)	^{78}Kr	^{80}Kr	^{82}Kr	^{83}Kr	^{86}Kr	
							$^{84}\text{Kr} = 100$
CG1	600	0.6079 ± 0.0043	3.926 ± 0.027	20.061 ± 0.041	20.033 ± 0.056	30.619 ± 0.077	
	800	0.5967 ± 0.0070	3.904 ± 0.030	20.138 ± 0.049	19.967 ± 0.058	30.395 ± 0.094	
	1000	0.6004 ± 0.0054	3.919 ± 0.030	19.931 ± 0.059	19.918 ± 0.067	30.434 ± 0.096	
	1200	0.5865 ± 0.0060	3.883 ± 0.029	20.291 ± 0.061	20.082 ± 0.071	30.541 ± 0.096	
	1400	0.586 ± 0.011	3.854 ± 0.042	20.359 ± 0.088	20.267 ± 0.090	30.59 ± 0.12	
	1600	0.5787 ± 0.0075	3.808 ± 0.039	20.135 ± 0.061	20.159 ± 0.073	30.70 ± 0.10	
	1800-1	1.3	0.5853 ± 0.0094	3.768 ± 0.059	20.03 ± 0.10	19.98 ± 0.11	30.60 ± 0.14
	1800-2	0.48	0.600 ± 0.019	3.670 ± 0.065	18.78 ± 0.16	19.86 ± 0.18	30.36 ± 0.18
	total	62	0.6002 ± 0.0026	3.905 ± 0.015	20.067 ± 0.025	20.016 ± 0.031	30.540 ± 0.044
	Terrestrial air		0.67	4.008	20.36	20.25	30.74
HL ^c		0.43	3.08	16.00	19.93	36.03	

Table 2a. Noble gas amounts and isotopic ratios of hot blanks.

Sample	Temp. (°C)	^{78}Kr	^{80}Kr	^{82}Kr	^{83}Kr	^{86}Kr
800	0.35	0.6087 ± 0.0046	3.960 ± 0.036	19.61 ± 0.66	18.1 ± 1.1	27.19 ± 0.82
1800	2.9	0.6087 ± 0.0046	3.98 ± 0.24	21.21 ± 0.40	19.59 ± 0.26	31.68 ± 0.42

^aGas concentrations are in units of 10⁻¹⁰ cm³STP/g.

^bHuss et al. (1996).

^cHuss and Lewis (1994b).

Table 3. Xenon in graphite nodule CG1 (359.97 mg) of Canyon Diablo.

Sample	Temp. (°C)	[¹³⁰ Xe] ^a	¹³⁰ Xe=100							
			¹²⁴ Xe	¹²⁶ Xe	¹²⁸ Xe	¹²⁹ Xe	¹³¹ Xe	¹³² Xe	¹³⁴ Xe	¹³⁶ Xe
CG1	600	59	2.298 ± 0.088	2.12 ± 0.10	47.99 ± 0.66	943.3 ± 4.9	522.0 ± 3.6	660.3 ± 3.9	255.6 ± 1.6	215.8 ± 1.4
	800	18	2.43 ± 0.10	2.24 ± 0.13	47.80 ± 0.70	1538.3 ± 8.6	518.8 ± 3.9	653.1 ± 4.3	249.3 ± 2.0	211.1 ± 1.6
	1000	41	2.408 ± 0.099	2.21 ± 0.11	48.89 ± 0.66	1815.4 ± 9.7	514.3 ± 3.7	644.2 ± 3.9	247.1 ± 1.6	208.1 ± 1.4
	1200	22	2.45 ± 0.12	2.30 ± 0.12	48.54 ± 0.75	2076 ± 14	514.8 ± 4.5	643.1 ± 4.7	246.2 ± 2.1	207.3 ± 1.8
	1400	14	2.47 ± 0.11	2.19 ± 0.11	47.72 ± 0.68	1975 ± 12	518.4 ± 4.0	648.2 ± 4.1	247.9 ± 1.7	208.8 ± 1.6
	1600	13	2.50 ± 0.12	2.36 ± 0.13	48.36 ± 0.76	2127 ± 15	516.6 ± 4.9	639.5 ± 4.9	245.3 ± 1.8	205.4 ± 1.8
	1800-2	4.1	2.68 ± 0.16	2.55 ± 0.15	49.07 ± 0.83	2860 ± 27	515.0 ± 5.1	635.2 ± 7.0	240.0 ± 2.8	203.4 ± 2.5
	total	170	2.397 ± 0.045	2.213 ± 0.052	48.29 ± 0.31	1579 ± 25	518.0 ± 1.8	650.3 ± 1.9	249.92 ± 0.83	210.71 ± 0.72
El Taco Xe ^b		2.554	2.325	48.55	≤750	514.4	648.7	249.3	209.0	
Modified El Taco Xe ^c		2.52	2.30	—	—	515.0	650.6	248.5	208.2	
Q ^d		2.87	2.54	50.9	638.0	503.8	613.5	231.8	194.2	
HL ^e		5.45	3.69	58.6	683.9	546.8	647.7	412.0	453.4	
Terrestrial air		2.337	2.180	47.15	649.6	521.3	660.7	256.3	217.6	

^aGas concentrations are in units of 10⁻¹² cm³STP/g. The first step of 1800 °C was lost because of the failure of software to detect peaks. The amounts of ¹³⁰Xe in this step is estimated to be less than that in 1600 °C fraction, and would not give severe effect on the total data (less than 10%).

^bMathew and Begemann (1995).

^cMaruoka (1999).

^dHuss et al. (1996).

^eHuss and Lewis (1994b).

The hot blanks of 800 °C and 1800 °C are 9.9 × 10⁻¹⁵ cm³STP and 8.0 × 10⁻¹⁴ cm³STP, respectively. As for the isotopic ratios, we assumed the air values.

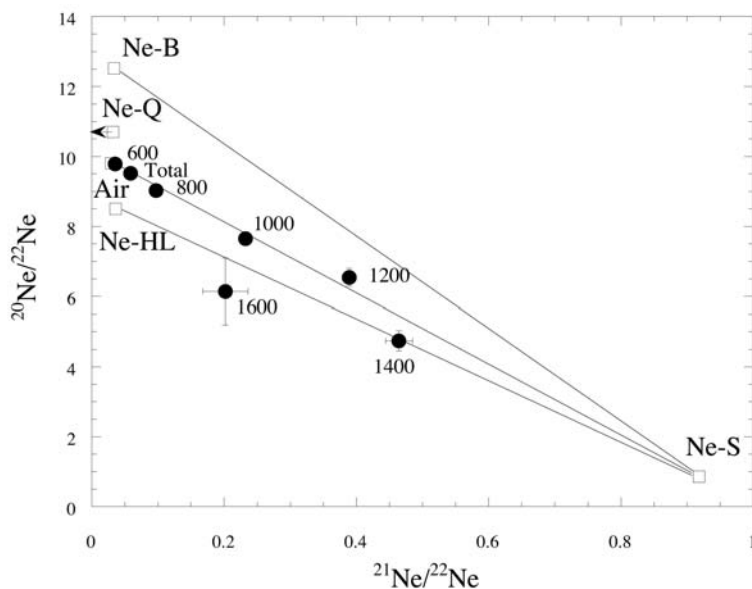


Fig. 2. Ne three-isotope plot of $^{20}\text{Ne}/^{22}\text{Ne}$ versus $^{21}\text{Ne}/^{22}\text{Ne}$ ratios. The numerical values are extraction temperatures of the stepwise heating. Ne-B is the solar component (Black 1972), Ne-Q, Ne-HL and air are from Table 1. Ne-S is the spallogenic component produced by cosmic ray spallation. The data points of the 600–1200 °C fractions lie on the mixing line between air and spallogenic component, but those of 1400 and 1600 °C lie on the mixing line of Ne-HL and spallogenic component. There seems to be no contribution by the solar component.

fractions are, if anything, upper limits, as the large hot blank correction tends to increase the $^{20}\text{Ne}/^{22}\text{Ne}$ ratio as stated before. The errors of the isotopic ratios include the errors of the linear regression at the measurement, discrimination corrections, and blank corrections. The error of the linear regression at the measurement is very small compared to that of the blank correction in 1400 and 1600 °C fractions. Thus, large errors of isotopic ratios of 1600 °C fraction are due to the blank correction. The variations of the isotopic ratios of the hot blank before and after the sample measurement were taken into the calculation.

The observed Ne-HL at high temperature fractions means the Ne-HL component is released at high temperatures after the air component had degassed at low temperatures. Spallogenic Ne is produced by cosmic ray reactions from elements with masses higher than that of Ne. Neon can not be produced by spallation from carbon, because the atomic mass of carbon is lower than that of Ne. However, some trace elements with higher mass may be present in the graphite, or a minor phase like cohenite ((Fe, Ni)₃C) could be the target. The spallogenic component was released in all temperature steps. Here, it should be emphasized that the linear array of data points of the 1400 and 1600 °C fractions implies that the primordial component of Ne is Ne-HL rather than solar Ne or Ne-Q. This suggests that pre-solar diamonds (the host phase of Ne-HL) were also incorporated into the graphite nodule of the Canyon Diablo iron meteorite just as they were trapped by carbonaceous chondrites and unequilibrated ordinary chondrites. It is interesting that there is no solar component of Ne in the graphite nodule, which is compatible with the results of Namba et al. (2000) whose Ne data of an acid

residue of Canyon Diablo fall between atmospheric Ne and planetary Ne, suggesting that the primordial component of the noble gases in Canyon Diablo carbon is planetary rather than solar.

The $^3\text{He}/^4\text{He}$ ratios in the graphite nodule are higher than those of He-Q or He-HL by an order of magnitude, indicating a contribution by a spallogenic component, which is also compatible with the Ne data.

Argon

The Ar data are shown in Fig. 3. The $^{40}\text{Ar}/^{36}\text{Ar}$ ratios of all the temperature release fractions were lower than that of the terrestrial atmosphere and there is no excess of ^{40}Ar . The interesting feature is the $^{38}\text{Ar}/^{36}\text{Ar}$ ratio which is higher than that of air except for 600 °C and the second 1800 °C fractions. This is due to spallation effects and/or the contribution by Ar-HL. However, it should be noted that the high $^{38}\text{Ar}/^{36}\text{Ar}$ ratios in the 1400 and 1600 °C fractions cannot be explained by the addition of spallogenic Ar only. When we estimated the amount of spallogenic Ar from the Ne isotopic ratios by assuming the relative ratio of spallogenic Ar and Ne in individual steps (the $^{38}\text{Ar}/^{21}\text{Ne}$ ratio is about 0.2 for carbonaceous chondrites and about 4–6 for irons; Mazor et al. 1970 and Voshage 1982), we could conclude that the high $^{38}\text{Ar}/^{36}\text{Ar}$ ratios in the 1400 and 1600 °C fractions are not explained by spallogenic Ar only, indicating the presence of Ar-HL in these temperature fractions. As the cosmogenic Ne is released at the temperatures lower than those for cosmogenic Ar, we might have compared the total amounts of cosmogenic ^{38}Ar and ^{21}Ne . The cosmogenic $^{38}\text{Ar}/^{21}\text{Ne}$ ratio in

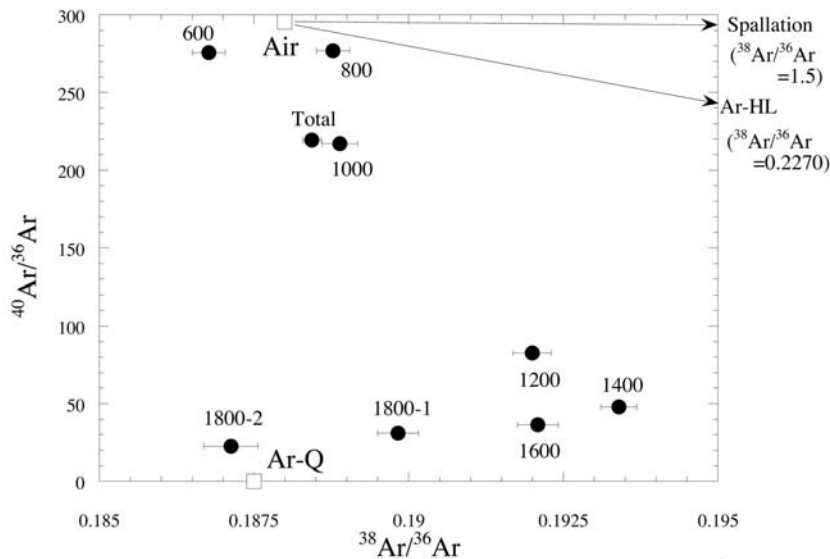


Fig. 3. Ar three isotope plot of $^{40}\text{Ar}/^{36}\text{Ar}$ versus $^{38}\text{Ar}/^{36}\text{Ar}$ ratios. The numerical values are extraction temperatures. Ar-Q, Ar-HL and air are from Table 1. The data points are distributed below the mixing line between air and Ar-HL (and spallogenic component), indicating the presence of Ar-Q in the graphite nodule.

all the temperature fractions in this sample is about 4.4. This ratio of 4.4 is still high when we consider that our sample is a graphite residue of metal-graphite inclusion and that the cosmogenic $^{38}\text{Ar}/^{21}\text{Ne}$ ratio of carbonaceous chondrites is about 0.2 and only in iron meteorites does it reach 4–6.

Furthermore, it is notable that the Ar data points plot below the mixing line between air and Ar-HL (and also below that between air and the spallogenic component), and seem to be situated inside the triangular area defined by the isotopic compositions of air, Ar-HL (and spallogenic component) and a third component. The third component is characterized by low $^{40}\text{Ar}/^{36}\text{Ar}$ and air-like $^{38}\text{Ar}/^{36}\text{Ar}$ ratios. Such a component is considered to be Ar-Q. Thus, the Ar data cannot be explained by a mixture of air and Ar-HL (and spallogenic Ar) alone and indicate the presence of Ar-Q. As the Ne concentration in Q is very low, it is likely that the presence of Ne-Q could not be identified in the Ne data. As the $^{20}\text{Ne}/^{36}\text{Ar}$ ratios of Q are 0.01–0.08 (Busemann et al. 2000), the ^{20}Ne -Q amount calculated from the estimated ^{36}Ar -Q is at most 2.5–20% of the total ^{20}Ne . The scattering of $^{38}\text{Ar}/^{36}\text{Ar}$ ratios at high temperature steps suggests that Q and HL components preserve isotopic inhomogeneity and are not located in a single phase produced by secondary igneous processes. This suggests that the graphite nodule was not exposed to high temperatures necessary for igneous processes.

Here it is noted that the low $^{38}\text{Ar}/^{36}\text{Ar}$ ratio of the 600 °C fraction is not explained by the mixture of air, spallogenic Ar, Ar-HL, and Ar-Q. This is not due to the remaining HCl from the HCl treatment to dissolve metal. The $^{37}\text{Cl}/^{35}\text{Cl}$ ratio (thus $^{38}\text{HCl}/^{36}\text{HCl}$ ratio) is about 0.3, higher than the air value (0.188), and the addition of the HCl would increase the $^{38}\text{Ar}/^{36}\text{Ar}$ ratio from the air value. Furthermore, it is likely that HCl

is easily evaporated at 100 °C. We suppose that the 600 °C fraction is the mixture of the adsorbed isotopically-fractionated air and some spallogenic component. The $^{40}\text{Ar}/^{36}\text{Ar}$ ratio of the 600 °C fraction is also low, and the $^{38}\text{Ar}/^{36}\text{Ar}$ ratio corresponding to this low $^{40}\text{Ar}/^{36}\text{Ar}$ ratio is lower than the observed value if we assume the simple mass fractionation process. The estimated amount of accompanying spallogenic ^{38}Ar is compatible with the spallogenic Ne amount when we estimated it from the Ne data and the $^{38}\text{Ar}/^{21}\text{Ne}$ ratio.

Krypton and Xenon

We could not observe noticeable excesses of ^{80}Kr and ^{82}Kr produced by neutron irradiation of bromine, which were often reported from inclusions in iron meteorites (Alexander and Manuel 1967; Mathew and Begemann 1995). We observed a large excess of ^{129}Xe , supposed to be the decay product of the extinct nuclide ^{129}I , as already suggested by Alexander and Manuel (1967, 1968) and Meshik et al. (2004). The $^{129}\text{Xe}/^{130}\text{Xe}$ ratio is higher than that of the terrestrial atmosphere in all temperature fractions (Fig. 4). The large excess of ^{129}Xe is considered as a decay product of the extinct nuclide ^{129}I . The cosmic ray exposure age of Canyon Diablo is estimated to be 610–675 Myr. (Voshage and Feldmann 1979). If the excess of ^{129}Xe is due to the cosmogenic irradiation, there should be high $^{128}\text{Xe}/^{130}\text{Xe}$ ratios, too (Murty and Marty 1987). Our data does not show such a trend. We can also deny the possibility of the neutron capture effect of Te, because there is no correlation between the $^{129}\text{Xe}/^{130}\text{Xe}$ and $^{131}\text{Xe}/^{130}\text{Xe}$ ratios.

Thus, the large excess of ^{129}Xe observed in the Canyon

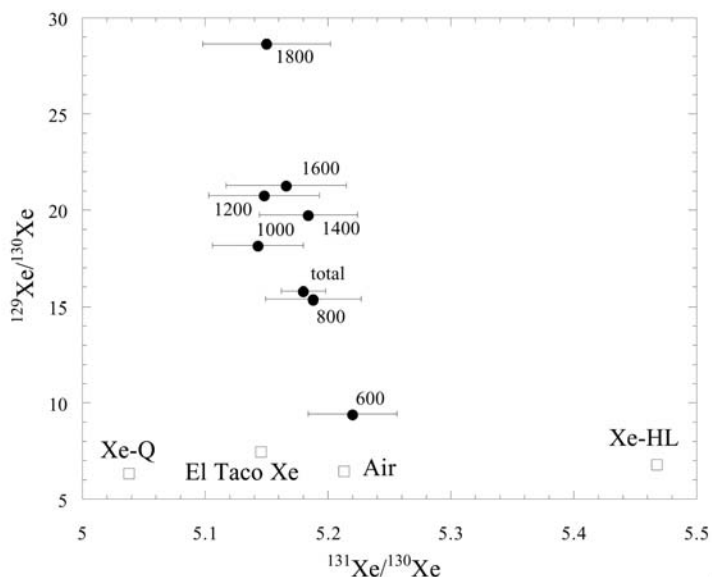


Fig. 4. $^{129}\text{Xe}/^{130}\text{Xe}$ versus $^{131}\text{Xe}/^{130}\text{Xe}$ ratios diagram. The numerical values are extraction temperatures of the stepwise heating. Xe-Q, Xe-HL, air and El Taco Xe are from Table 1. The modified El Taco Xe is almost at the same position of El Taco Xe in this and subsequent figures. There are excesses of ^{129}Xe in fractions of all temperature steps for the graphite-metal inclusion of Canyon Diablo indicating locations of very high temperature stability.

Diablo graphite-metal inclusion indicates that the graphite was formed while ^{129}I was still present. The amount of excess ^{129}Xe is about 1.7×10^{-9} cm³STP/g which corresponds to about 7.6×10^{-14} mol/g or 1×10^{-11} g/g (0.00001 ppm) ^{129}I . If $^{129}\text{I}/^{127}\text{I}$ was about 10^{-4} (Ozima and Podosek 2002), the ^{127}I concentration would have been about 0.1 ppm, about 0.2 times the abundance in CI chondrites. It is perhaps possible that the graphite contains such a small amount of I, but it is rather likely that some minor I-rich minerals were disseminated in the graphite. This view is supported by the omnipresent Cl-rich rust that develops everywhere on freshly cut surfaces of the CDGrMet sample, indicating the presence of lawrencite (FeCl_2), which could be the carrier of I. The I-bearing lawrencite is certainly a low-temperature mineral, the presence of which may indicate that the graphite-metal inclusion was not heated to high temperatures, neither during its formation, nor during its incorporation into the metal.

Now we will discuss the primordial component of Xe. The Xe data are plotted in the $^{134}\text{Xe}/^{130}\text{Xe}$ versus $^{136}\text{Xe}/^{130}\text{Xe}$ ratios diagram (Fig. 5). We also plotted carbonaceous chondrites and ureilites data in the same figure. These data points are distributed around Xe-Q and on the mixing line between Xe-Q and Xe-HL. All data points from the Canyon Diablo graphite lie on the mixing line between air and Xe-Q and there seems to be a negligible contribution from Xe-HL. This may seem curious but is compatible with the Ar data and also with the Ne data that show the contribution from the HL component at high temperatures only. The ^{132}Xe content in Q is one to two orders of magnitude higher than that of Xe-HL (Huss et al. 1996) and the $^{132}\text{Xe}/^{20}\text{Ne}$ ratio in Q is about two orders of magnitude higher than that of HL (Wieler et al.

1991). Thus, it is very likely that only the contribution of Q can be seen in the Xe data. Another interesting feature is that our data points are on the extrapolated side of the mixing line between air and El Taco Xe, which is very different from the Xe data obtained from the graphite residues from the El Taco IAB iron by Mathew and Begemann (1995). The El Taco Xe was defined as one end member in the same diagram of $^{134}\text{Xe}/^{130}\text{Xe}$ versus $^{136}\text{Xe}/^{130}\text{Xe}$ ratios as Fig. 5. Our data seem to show that Q, rather than El Taco Xe, is responsible for one end member of the mixing line. Another end member of the mixing line for the graphite residues of El Taco in Mathew and Begemann (1995) was air, which is the same as the data in this study.

However, it is not certain whether El Taco Xe could be an end member or not in Fig. 5, because El Taco Xe is on the mixing line between air and Q in this diagram. It is very likely that both Q and El Taco Xe could be the end members. We realized that El Taco Xe is always situated near the mixing line between air and Q in almost all diagrams of different combinations of Xe isotopes as long as we used the ^{130}Xe -normalized data. The isotope ^{130}Xe is generally used for the normalization of xenon isotopes because this isotope is free from fissionogenic contribution, which is useful when we discuss these effects, but we sometimes use ^{132}Xe for the normalization, because ^{132}Xe is the most abundant isotope.

Thus we used ^{132}Xe -normalized data and plotted them in a $^{130}\text{Xe}/^{132}\text{Xe}$ versus $^{136}\text{Xe}/^{132}\text{Xe}$ ratios (Fig. 6a) and in a $^{131}\text{Xe}/^{132}\text{Xe}$ versus $^{136}\text{Xe}/^{132}\text{Xe}$ ratios diagram (Fig. 6b). In these diagrams, Q, air and El Taco Xe are not on a single line but form a triangle. Thus, we can clearly detect the presence of El Taco Xe. Xe-HL is far on the right side of this diagram

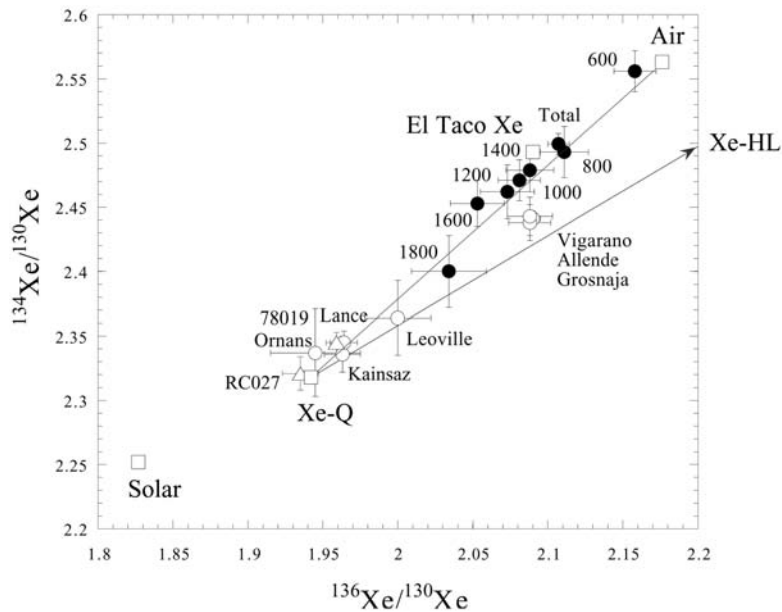


Fig. 5. $^{134}\text{Xe}/^{130}\text{Xe}$ versus $^{136}\text{Xe}/^{130}\text{Xe}$ ratios diagram. The numerical values are extraction temperatures of the stepwise heating. Xe-Q, Xe-HL, air and El Taco Xe are from Table 1. Solar is the surface-correlated Xe (solar wind Xe) in lunar soils (Podosek et al. 1971). We also plotted the Xe data of CV chondrites Allende (Srinivasan et al. 1978), Vigarano (Matsuda et al. 1980), Grosnaja (Matsuda et al. 1980), Leoville (Manuel et al. 1970), CO chondrites Lancé (Alaerts et al. 1979), Kainsaz (Alaerts et al. 1979), Ornans (Mazor et al. 1970) and ureilites (78019 is the ALH A78019 (Wacker 1986) and RC027 the Roosevelt County 027 (Goodrich 1987)). The data points from the graphite-metal inclusion of Canyon Diablo seem to lie on the mixing line between air and Xe-Q.

because of its high $^{136}\text{Xe}/^{132}\text{Xe}$ ratio (0.6991). The Xe data of Canyon Diablo plot inside the triangle of Q, air and El Taco Xe, and clearly show the presence of El Taco Xe. This is also true for other IAB irons such as Toluca (Hennecke and Manuel 1977) and Bohumilitz (Maruoka et al. 2001; see Fig. 7 in Maruoka et al. 2001). This is quite different from the graphite data of the El Taco IAB iron where the contribution of Q is not observed and the data mainly plot between air and El Taco Xe in the diagram with ^{130}Xe normalization (Mathew and Begemann 1995).

Thus, all IAB iron meteorites measured so far have El Taco Xe, Q and air. There is a negligible contribution of Xe-HL, and the contribution by Xe-Q is different in individual IAB irons. Maruoka (1999) identified the contributions of Xe-Q and Xe-HL in El Taco Xe itself and redefined the new El Taco Xe from the precise data reduction using ^{132}Xe normalization. In this sense, the El Taco mass of the Campo del Cielo meteorite also contains Xe-Q and Xe-HL, but their contributions are very small compared with other IAB irons (Canyon Diablo in this study, Toluca and Bohumilitz). The contribution by Xe-HL is difficult to detect even in the latter IAB irons. This is because the Xe/Ne ratio is low in the HL component as we already mentioned above. The Xe data of ureilites are close to Xe-Q and those of carbonaceous chondrites are on and below the mixing line between Q and HL. The reason why the data plot below the mixing line is the addition of air or El Taco Xe, but we cannot identify the third component. As long as we are fixed to the idea that a

considerable contribution from air is present, we do not consider the presence of El Taco Xe. At any rate, the data of Canyon Diablo graphite plot into a region that is very much different from that of carbonaceous chondrites and clearly shows the presence of El Taco Xe.

THE NOBLE GAS SIGNATURES OF THE CD GRAPHITE-METAL INCLUSION AND THEIR IMPLICATIONS

It is astonishing and interesting that the noble gas signatures of graphite from the graphite-metal inclusion are comparable to those of carbonaceous chondrites but differ from them in some features:

1. The HL/Q ratios of graphite inclusions from the Canyon Diablo iron are low compared with those of carbonaceous chondrites. Thus, we could not detect the HL component from Xe isotopic data in spite of the fact that Xe-HL is clearly observed in carbonaceous chondrites. This may suggest that the HL component in the graphite-metal inclusion of Canyon Diablo was damaged by some process. One plausible process is some kind of thermal metamorphism. Huss et al. (1996) observed a systematic difference in the abundances of various noble gas components, such as HL and Q, in non-metamorphosed, unequilibrated chondrites of different classes (type 3) and concluded that the host phase Q is more resistant to metamorphic degassing than

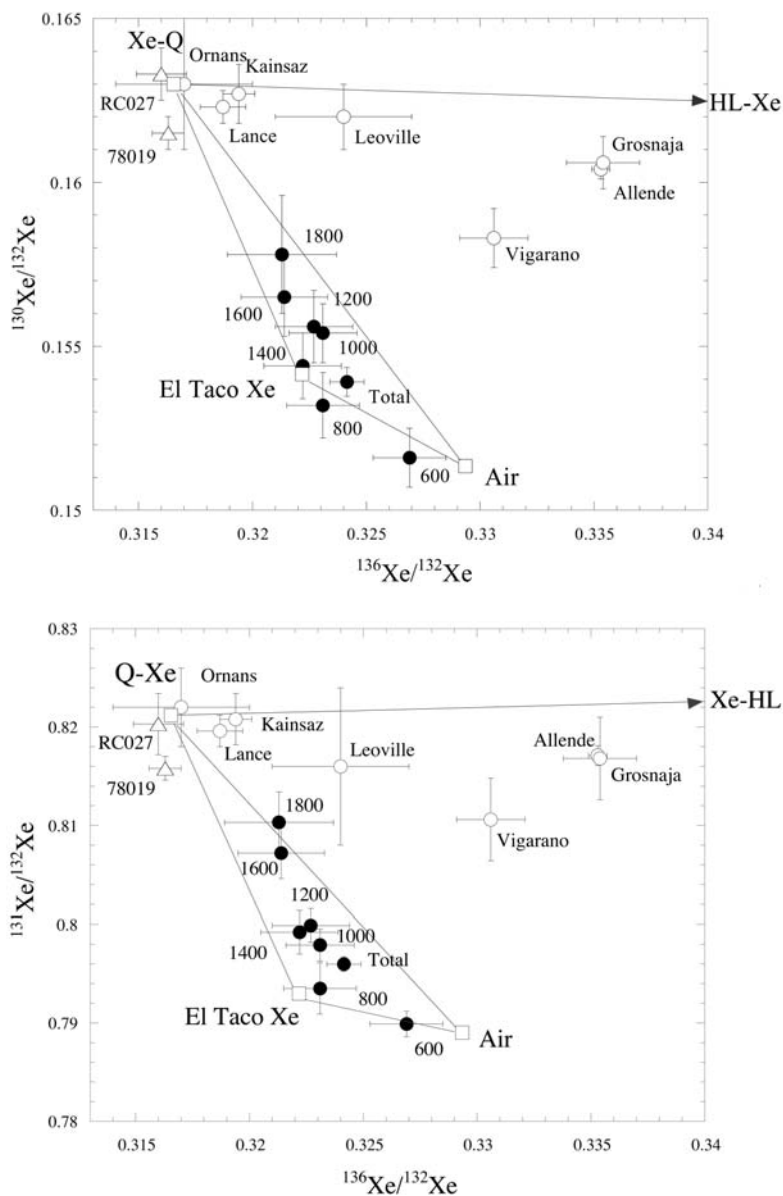


Fig. 6. a) $^{130}\text{Xe}/^{132}\text{Xe}$ versus $^{136}\text{Xe}/^{132}\text{Xe}$ ratios and b) $^{131}\text{Xe}/^{132}\text{Xe}$ versus $^{136}\text{Xe}/^{132}\text{Xe}$ ratios diagrams. All the numerical values and symbols are the same as given in Fig. 5. The presence of El Taco Xe in the graphite-metal inclusion of Canyon Diablo is clearly evident in these diagrams.

diamond (the host phase of HL). The HL component is almost zero even in Julesburg (L3.7) where not even the Ne data do show the presence of Ne-HL (Fig. 11 in Huss et al. 1996). In our study, the Ne-HL seems to be still observed in the graphite-metal inclusion of Canyon Diablo. Thus, we can estimate that the temperature for the thermal metamorphism for the graphite-metal inclusion of Canyon Diablo was not as high as that for a type 3.7 ordinary chondrite. Thus, the temperature of metamorphism is estimated to be about 500–600 °C (McSween 1999).

- So far, El Taco Xe seems to be present in iron meteorites only and has not been found in carbonaceous chondrites.

The data of some carbonaceous chondrites cannot be explained by mixing of Q and HL alone. However, the presence of HL makes it difficult to identify the third component; air or El Taco Xe.

Maruoka (1999) discussed the origin of El Taco Xe and concluded that El Taco Xe as proposed by Mathew and Begemann (1995) contains Q and HL with a HL/Q ratio higher than that in primitive chondrites. Thermal metamorphism has to be excluded as a possible process, because it selectively damages HL and produces a low HL/Q ratio, which is just the opposite to that observed in El Taco Xe. Shock-loading experiment indicate that Q is preferentially lost up to a total loss of 75% of noble gases

without damaging HL at 70 GPa (Nakamura et al. 1997). However, there is no evidence that El Taco graphite had experienced such a high pressure in the past. Thus, Maruoka (1999) concluded that the HL/Q ratio of the El Taco graphite might be originally different from that observed in primitive chondrites. Recently, Matsuda et al. (Forthcoming) found that the resistance of the carrier of Q is weaker than that of HL against aqueous alteration, which is just the opposite to the thermal metamorphism. They kept Allende in a pressure vessel with pure water at 200 °C for two and four weeks. After four weeks, Q decreased to 60% but there was no significant effect on HL. Thus, one of the possible explanations for the low Q/HL ratio observed in EL Taco graphite is the effect of aqueous alteration or an equivalent process. Maruoka (1999) redefined the “modified El Taco Xe” as the indigenous component with the HL and Q components removed from the original “El Taco Xe” as proposed by Mathew and Begemann (1995). The isotopic signature of “modified El Taco Xe” is well explained by the mass-dependent fractionation from the solar Xe or U-Xe (Maruoka 1999).

Another important feature of noble gases in this study is the presence of an atmosphere-like component at high temperatures. This may suggest that the atmosphere-like component exists as one of primordial components in iron meteorites. This atmosphere-like component is often observed at the noble gas measurement of iron meteorite, as stated before in the Introduction. In the case of the iron sample, we can not rule out the possibility that this air was liberated from the crucible through the reaction of the sample and the crucible (Matsuda et al. 1996; Maruoka and Matsuda 2001). The iron can surely react with the crucible, but it is not certain whether graphite reacts with the Ta crucible or not. Although it is very interesting if the atmosphere-like component is one of the main components of noble gases in iron, further studies are necessary to confirm it.

CONCLUSIONS

We have drawn the following conclusions from the stepwise heating experiment of noble gases in the graphite CG1 from Canyon Diablo’s graphite-metal inclusion CDGrMet:

1. The graphite-metal inclusion contains various kinds of noble gas components: Q, HL and El Taco Xe, although the presence of HL seemed to be confirmed in light noble gases (Ne and Ar) only. These components seem to be commonly present in almost all IAB iron meteorites although Q is missing in the El Taco mass of Campo del Cielo. The presence of these components indicates that the graphite-metal inclusion was not heated to igneous temperatures. The HL/Q ratios in the graphite-metal inclusion in Canyon Diablo are lower than those of carbonaceous chondrites, indicating that the graphite-

metal inclusion was heated at most to about 500–600 °C. At these temperatures only HL is damaged, but Q is not. Here, we should also note that the evidence of Ne-HL and Ar-HL is not so strong and it is also likely that there is no HL component at all in this sample.

2. “El Taco Xe” is observed in almost all IAB iron meteorites, but it has not been identified with certainty in carbonaceous chondrites. El Taco Xe seems to be a specific component of iron meteorites. El Taco Xe itself, as originally defined, contains some Q and HL, and its HL/Q ratio is higher than that of carbonaceous chondrites. One of the possible explanations for this is an aqueous alteration, to which Q is less resistant than HL.
3. A large excess of ^{129}Xe exists, which is supposed to be the decay product from the extinct nuclide ^{129}I , indicating that the graphite-metal inclusion was formed in the early stage of the solar nebula while ^{129}I was still present.
4. It is likely that an atmosphere-like component is one of main phases of noble gases in iron meteorite, but further studies are necessary to confirm it.

Our results place tight constraints on models for the origin of the graphite-metal inclusions in the Canyon Diablo iron and IAB iron meteorites. Our data indicate that the graphite-metal inclusion CDGrMet was formed in a primitive, probably nebular, environment and was trapped by the metal at low, subsolidus temperatures very early in the history of the solar system, which is in agreement with the recently proposed low-temperature origin of iron meteorites (Kurat et al. 2000; Kurat 2003; Maruoka et al 2003).

Acknowledgments—This work was supported by Austrian FWF (G. Kurat) and by a Research Fellowship of the Japanese Society for the Promotion of Science for the Young Scientists (T. Maruoka). We thank also Dr. Alex Meshik and Dr. Susanne Schwenzer for their critical and constructive reviews. Thanks are also to Dr. Timothy D. Swindle for his careful editing and suggestions as a handling editor.

Editorial Handling—Dr. Timothy Swindle

REFERENCES

- Alaerts L., Lewis R. S., and Anders E. 1979. Isotopic anomalies of noble gases in meteorites and their origins. IV—C3 Orns carbonaceous chondrites. *Geochimica et Cosmochimica Acta* 43: 1421–1432.
- Alexander E. C. Jr. and Manuel O. K. 1967. Isotopic anomalies of krypton and xenon in Canyon Diablo graphite. *Earth and Planetary Science Letters* 2:220–224.
- Alexander E. C. Jr. and Manuel O. K. 1968. Xenon in the inclusions of Canyon Diablo and Toluca iron meteorites. *Earth and Planetary Science Letters* 4:113–117.
- Amari S., Zaizen S., and Matsuda J. 2003. An attempt to separate Q from the Allende meteorite by physical method. *Geochimica et Cosmochimica Acta* 67:4665–4677.

- Black D. C. 1972. On the origins of trapped helium, neon and argon isotopic variations in meteorites I. Gas-rich meteorites, lunar soil and breccia. *Geochimica et Cosmochimica Acta* 36:347–375.
- Busemann H., Baur H., and Wieler R. 2000. Primordial noble gases in “phase Q” in carbonaceous and ordinary chondrites studied by closed-system stepped etching. *Meteoritics & Planetary Science* 35:949–973.
- Fisher D. E. 1981. A search for primordial atmospheric-like argon in an iron meteorite. *Geochimica et Cosmochimica Acta* 45:245–249.
- Goodrich C. A., Keil K., Berkley J. L., Laul J. C., Smith M. R., Wacker J. F., Clayton R. N., and Mayeda T. K. 1987. Roosevelt County 027—A low-shock ureilite with interstitial silicates and high noble gas concentrations. *Meteoritics* 22:191–218.
- Hennecke E. W. and Manuel O. K. 1977. Argon, krypton, and xenon in iron meteorites. *Earth and Planetary Science Letters* 36:29–43.
- Huss G. R. and Lewis R. S. 1994a. Noble gases in presolar diamonds I: Three distinct components and their implications for diamond origin. *Meteoritics* 29:791–810.
- Huss G. R. and Lewis R. S. 1994b. Noble gases in presolar diamonds II: Component abundances reflect thermal processing. *Meteoritics* 29:811–829.
- Huss G. R., Lewis R. S., and Hemkin S. 1996. The “normal planetary” noble gas component in primitive chondrites: Compositions, carrier, and metamorphic history. *Geochimica et Cosmochimica Acta* 60:3311–3340.
- Hwaung G. and Manuel O. K. 1982. Terrestrial-type xenon in meteoritic troilite. *Nature* 299:807–810.
- Kurat G. 2003. Why iron meteorites cannot be samples of planetesimal smelting (abstract). Symposium, Evolution of Solar System Materials: A New Perspective from Antarctic Meteorites. pp. 65–66.
- Kurat G., Sylvester P., Kong P., and Brandstätter F. 2000. Heterogeneous and fractionated metal in Canyon Diablo (IA) graphite-metal rock (abstract #1666). 31st Lunar and Planetary Science Conference. CD-ROM.
- Manuel O. K., Wright R. J., Miller D. K., and Kuroda P. K. 1970. Heavy noble gases in Leoville: The case for mass fractionated xenon in carbonaceous chondrites. *Journal of Geophysical Research* 75:5693–5701.
- Maruoka T. 1999. Re-definition of “El Taco Xe” based on ¹³²Xe-normalized data: Multiple primordial components in IAB irons. *Geochemical Journal* 33:343–350.
- Maruoka T. and Matsuda J. 2001. New crucible for noble gas extraction. *Chemical Geology* 175:751–756.
- Maruoka T., Matsuda J., and Kurat G. 2001. Abundance and isotopic composition of noble gases in metal and graphite of the Bohumilitz IAB iron meteorite. *Meteoritics & Planetary Science* 36:597–609.
- Maruoka T., Kurat G., Zinner E., Varela M. E., and Ametrano S. J. 2003. Carbon isotopic heterogeneity of graphite in the San Juan mass of the Campo del Cielo IAB iron meteorite (abstract #1663). 34th Lunar and Planetary Science Conference. CD-ROM.
- Mathew K. J. and Begemann F. 1995. Isotopic composition of xenon and krypton in silicate-graphite inclusions of the El Taco, Campo del Cielo, IAB iron meteorite. *Geochimica et Cosmochimica Acta* 59:4729–4746.
- Matsuda J., Lewis R. S., Takahashi H., and Anders E. 1980. Isotopic anomalies of noble gases in meteorites and their origins. VII—C3V carbonaceous chondrites. *Geochimica et Cosmochimica Acta* 44:1861–1874.
- Matsuda J., Matsubara K., Yajima H., and Yamamoto K. 1989. Anomalous Ne enrichment in obsidians and Darwin glass: Diffusion of noble gases in silica-rich glasses. *Geochimica et Cosmochimica Acta* 53:3025–3033.
- Matsuda J., Nagao K., and Kurat G. 1996. Noble gases in metal and schreibersite of the Acuña (IVAB) iron meteorite. *Meteoritics & Planetary Science* 31:227–233.
- Matsuda J., Yasuda T., Nakasyo E., and Matsumoto T. Forthcoming. Laboratory experiments on the effects of hydrothermal alteration on noble gases in the Allende CV3 chondrite. *Geochimica et Cosmochimica Acta*.
- Mazor E., Heymann D., and Anders E. 1970. Noble gases in carbonaceous chondrites. *Geochimica et Cosmochimica Acta* 34:781–824.
- McSween H.Y. Jr. 1999. *Meteorites and their parent planets*, 2nd ed. Cambridge: Cambridge University Press. 309 p.
- Meshik A., Kurat G., Pravdivstseva O., and Hohenberg C. M. 2004. Radiogenic ¹²⁹Xenon in silicate inclusions in the Campo del Cielo iron (abstract #1687). 35th Lunar and Planetary Science Conference. CD-ROM.
- Murty S. V. S. and Marti K. 1987. Nucleogenic noble gas components in the Cape York iron meteorite. *Geochimica et Cosmochimica Acta* 51:163–172.
- Nakamura T., Zolensky M.E., Hörz F., Takaoka N., and Nagao K. 1997. Impact-induced loss of primordial noble gases from experimentally soaked Allende meteorites (abstract). *Antarctic Meteorites* 22:135–136.
- Namba M., Maruoka T., Amari S., and Matsuda J. 2000. Neon isotopic composition of carbon residues from the Canyon Diablo iron meteorite. *Antarctic Meteorite Research* 13:170–176.
- Ozima M. and Podosek F. A. 2002. *Noble gas geochemistry*, 2nd ed. Cambridge: Cambridge University Press. 286 p.
- Podosek F. A., Huneke J. C., Burnett D. S., and Wasserburg G. J. 1971. Isotopic composition of xenon and krypton in the lunar soil and in the solar wind. *Earth and Planetary Science Letters* 10:199–216.
- Schultz L. and Kruse H. 1989. Helium, neon, and argon in meteorites: A data compilation. *Meteoritics* 24:155–172.
- Scott E. R. D. and Wasson J. T. 1975. Classification and properties of iron meteorites. *Reviews of Geophysics and Space Physics* 13:527–546.
- Shukolyukov Y. A., Minh D. V., Goel P. S., and Zaslavskaja N. I. 1984. Isotopic composition of xenon and krypton in micro- and macroinclusions in iron meteorites. *Geokhimiya* 6:771–780. In Russian.
- Srinivasan B., Lewis R. S., and Anders E. 1978. Noble gases in the Allende and Abee meteorites and a gas-rich mineral fraction—Investigation by stepwise heating. *Geochimica et Cosmochimica Acta* 42:183–198.
- Voshage H. 1982. Investigations of cosmic-ray-produced nuclides in iron meteorites. 4. Identification of noble gas abundance anomalies. *Earth and Planetary Science Letters* 61:32–40.
- Voshage H. and Feldmann H. 1978. Investigations on cosmic-ray-produced nuclides in iron meteorites. 1. The measurement and interpretation of rare gas concentrations. *Earth and Planetary Science Letters* 39:25–36.
- Wacker J. F. 1986. Noble gases in the diamond-free ureilite, ALH A78019. The roles of shock and nebular processes. *Geochimica et Cosmochimica Acta* 50:633–642.
- Wasson J. T. and Wang J. 1986. A non-magmatic origin of group IIE iron meteorites. *Geochimica et Cosmochimica Acta* 50:725–732.
- Wieler R., Baur H., Signer P., Anders E., and Lewis R. S. 1991. Noble gases in “phase Q”: Closed-system etching of an Allende residue. *Geochimica et Cosmochimica Acta* 55:1709–1722.